ARTICLES

Reconstitution of Rab- and SNARE-dependent membrane fusion by synthetic endosomes

Takeshi Ohya[1], Marta Miaczynska[1]†, Ünal Coskun[1], Barbara Lommer[1], Anja Runge[1], David Drechsel[1], Yannis Kalaidzidis[1,2] & Marino Zerial[1]

Rab GTPases and SNAREs (soluble *N*-ethylmaleimide-sensitive factor attachment protein receptors) are evolutionarily conserved essential components of the eukaryotic intracellular transport system. Although pairing of cognate SNAREs is sufficient to fuse membranes *in vitro*, a complete reconstitution of the Rab–SNARE machinery has never been achieved. Here we report the reconstitution of the early endosomal canine Rab5 GTPase, its key regulators and effectors together with SNAREs into proteoliposomes using a set of 17 recombinant human proteins. These vesicles behave like minimal 'synthetic' endosomes, fusing with purified early endosomes or with each other *in vitro*. Membrane fusion measured by content-mixing and morphological assays requires the cooperativity between Rab5 effectors and cognate SNAREs which, together, form a more efficient 'core machinery' than SNAREs alone. In reconstituting a fusion mechanism dependent on both a Rab GTPase and SNAREs, our work shows that the two machineries act coordinately to increase the specificity and efficiency of the membrane tethering and fusion process.

An outstanding question in the field of molecular cell biology is the functional relationship between Rab GTPases and SNAREs, key components of the intracellular trafficking apparatus[1–7]. Rab GTPases regulate the membrane recruitment and activity of tethering factors bringing together membranes compatible for fusion[2,3,8,9]. Membrane fusion is thought to be mediated by the formation of energetically stable *trans*-SNARE complexes engaging vesicle v-SNAREs (mostly R-SNAREs) and target t-SNAREs (mostly Q-SNAREs), enabling the closely apposed membranes to overcome the free energy barrier and fuse[4,5,10–12]. Because SNAREs can fuse membranes when reconstituted in proteoliposomes[4,5,10], they were proposed to be the core components of membrane fusion[10,13] and compartment specificity[5]. The original fusion reactions were inefficient, and required long times and non-physiological concentrations of SNAREs[5,10,13]. However, when SNAREs are in an assembled state, the transition from membrane docking to lipid mixing occurs in milliseconds[14,15]. Truncation of SNAREs enhances the efficiency and speed of membrane fusion[16,17], indicating that SNAREs contain regulatory domains that require other factors enabling their fusogenic activity. Moreover, other studies questioned the role of SNAREs as sole determinants of membrane fusion specificity[18]. This argues in favour of additional components regulating membrane fusion and compartmental specificity. Rab GTPases and their effectors are primary candidates for such a role.

Consistent with a function in determining the structural and functional identity of organelles, Rab GTPases and their effectors have a much narrower compartmental distribution[2,19,20] than SNAREs. On endosomes, assembly of the Rab5 domain involves a complex cascade of molecular interactions involving regulators of the nucleotide cycle (for example, rabaptin-5–rabex-5, a Rab5 effector–guanine nucleotide exchange factor (also termed rabaptin–RAB GEF 1) complex[21]) and Rab effectors. An important Rab5 effector is the phosphatidylinositol-3-OH kinase (PI(3)K) hVPS34 (also known as PIK3C3)–PIK3R4 (also known as p150) (refs 22, 23), which regulates the synthesis of phosphatidylinositol-3-phosphate (PtdIns(3)P)—a hallmark of early endosomes. Both Rab5 and PtdIns(3)P serve as binding sites for effectors required for membrane tethering and fusion (rabaptin-5–rabex-5 (ref. 21), early endosome antigen 1 (EEA1; ref. 8), rabenosyn-5 (also known as ZFYVE20)–hVPS45 (ref. 24), rabankyrin-5 (also known as ANKFY1; ref. 25)) through functional interactions with SNAREs[26] and intracellular motility[27]. Rab5-domain assembly and function therefore depends on cooperativity among Rab5 effectors and between these and SNAREs[2,28]. Here we reconstituted Rab5-domain assembly *in vitro*, with the intent of recapitulating membrane tethering and fusion, more faithfully and efficiently than SNAREs alone.

Rab effectors in early endosome fusion *in vitro*

A set of recombinant proteins, including Rab5, its interacting proteins and effectors[2] as well as the t- or Q-SNAREs syntaxin 13 (also known as syntaxin 12), VTI1A and syntaxin 6 and the v- or R-SNARE VAMP4 (refs 18, 26, 29) responsible for early endosomes fusion, were expressed either in *Escherichia coli* or Sf+ cells using the baculovirus expression system and purified (some partially, Supplementary Fig. 1 and Supplementary Table 1). First, we ensured that the purified proteins were active in an *in vitro* homotypic endosome fusion measured using a content mixing assay[21]. In brief, 'donor' endosomes purified from HeLa cells after internalization of biotinylated transferrin were mixed with 'acceptor' endosomes containing endocytosed anti-transferrin antibodies (Supplementary Fig. 2a). The biotinylated immunocomplexes were captured on streptavidin-coated plates and revealed using ruthenium labels that emit light when electrochemically stimulated (Meso Scale Discovery, MSD; see Methods). This electro-chemiluminescence system has the advantages of high sensitivity and dynamic range, as well as minimal background signals (Supplementary Fig. 2b, c). Addition of unlabelled transferrin in the

[1]Max Planck Institute of Molecular Cell Biology and Genetics, Pfotenhauerstrasse 108, 01309, Dresden, Germany. [2]A. N. Belozersky Institute of Physico-Chemical Biology, Moscow State University, Moscow 119899, Russia. †Present address: International Institute of Molecular and Cell Biology (IIMCB), Ks. Trojdena 4, 02-109 Warsaw, Poland.

reaction prevents the formation of labelled immunocomplexes resulting from leakage of markers upon membrane lysis, as observed for proteoliposomes[30,31] or yeast vacuoles[32]. Solubilization of membranes without unlabelled transferrin yields the total amount of immunocomplexes achievable in the assay (100% signal). The background in homotypic endosome fusion was estimated by solubilizing membranes without incubation and in the presence of unlabelled transferrin to be 4.6 ± 1.0% of the total signal and subtracted from each measurement. As a result, some values of the fusion activity presented in the graphs are negative within the range of 0–2%, the inherent variability of the system.

No significant fusion signal was detected when donor and acceptor endosomes were incubated with the ATP-regenerating system alone. The addition of cytosol (3 mg ml^{-1}) from HeLa cells enhanced fusion, which reached ~19% of the total signal (Fig. 1, compare lanes 1 and 2). We next attempted to substitute cytosol with the purified recombinant proteins added at concentrations similar to those provided by cytosol (see Supplementary Table 1). The concomitant addition of 50 nM recombinant prenylated Rab5–Rab guanine dissociation inhibitor (RabGDI) complex[33], 30 nM rabaptin-5–rabex-5 (ref. 21), 5 nM hVPS34–PIK3R4 (ref. 22), 100 nM EEA1 (ref. 8), rabenosyn-5–hVPS45 (ref. 24), rabankyrin-5 (ref. 25), 500 nM *N*-ethylmaleimide-sensitive factor (NSF) and soluble NSF attachment protein alpha (α-SNAP, also known as NAPA) required for the priming of *cis*-SNARE complexes[34] stimulated endosome fusion to an extent similar to cytosol (~19% versus 14%; Fig. 1, lanes 2 and 13). Selectively omitting individual components gave indications regarding their requirement for the fusion reaction (Fig. 1, lanes 3–12). For example, NSF and α-SNAP were essential. In contrast, omission of the Rab5–RabGDI complex produced relatively high fusion activity (Fig. 1, lane 6), although clearly lower than that stimulated by cytosol, probably due to residual native Rab5 and effectors on the purified endosomes (Supplementary Fig. 3), consistent with previous studies[22,35]. Exclusion of rabaptin-5–rabex-5, hVPS34–PIK3R4, EEA1 or rabenosyn-5–hVPS45 also generated minimal (~2–8%) fusion activity. Only removal of rabankyrin-5 did not decrease the fusion. Nevertheless, the recombinant protein is functional because

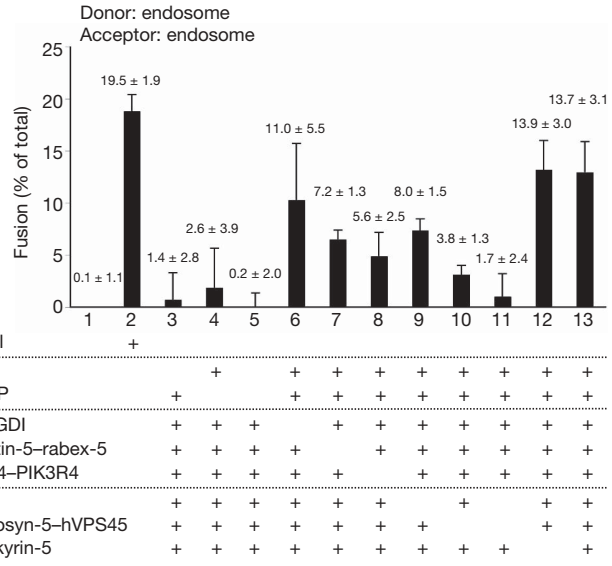

Figure 1 | Rab5 effectors and SNARE priming factors can substitute cytosol in the homotypic fusion between early endosomes *in vitro*. Homotypic early endosome fusion was carried out in the absence (lane 1) or presence of cytosol (lane 2) or the indicated combination of recombinant proteins at the concentration specified in Supplementary Table 1 (lanes 3–13) at 37 °C for 25 min. Fusion efficiency is expressed as percentage of the total possible fusion signal (see Methods). The precise values are indicated above each column. All data show the average of three independent experiments and s.e.m.

100 nM rabankyrin-5 stimulated the fusion reaction with cytosol by 25% (not shown, see ref. 25). We conclude that, with the exception of rabankyrin-5, all recombinant factors of the Rab5 machinery tested here are necessary and, together, sufficient for substituting cytosol in the early endosome fusion *in vitro*.

Recruitment of Rab5 and effectors on proteoliposomes

Next, we attempted to replace purified endosomes with proteoliposomes harbouring SNAREs complemented by the Rab5 machinery. To deliver prenylated Rab5 by RabGDI onto the membranes, we also implanted recombinant His_6-tagged prenylated Rab acceptor 1 (PRA1, also known as RABAC1), because this protein acts as a GDI displacement factor (GDF) primarily on Rab9, but also on Rab5 (ref. 36). Proteoliposomes were prepared by mixing recombinant proteins solubilized in detergent with lipids extracted from endosome fractions (to closely mimic the endosomal lipid composition) followed by dialysis of detergent and flotation on Histodenz density gradient (see Methods). Importantly, this protocol yielded a SNARE-to-phospholipid molar ratio similar to that of purified native endosomes (see syntaxin 13 in Fig. 2a, compare lanes 1–5 with 6). We then monitored the recruitment of Rab5, EEA1 and rabenosyn-5–hVPS45 onto these proteoliposomes by western blot analysis. Figure 2a shows that RabGDI delivered Rab5 on proteoliposomes containing PRA1 (compare lane 1 with 4). However, delivery of Rab5 alone was not sufficient for efficient membrane recruitment of EEA1 and rabenosyn-5, consistent with the dependence on Rab5 activation by GDP/GTP exchange (lane 2). Note that the amount of Rab5 recruited on the proteoliposomes in this case was low, presumably due to the counteracting extraction by RabGDI. Addition of the rabaptin-5–rabex-5 complex increased the membrane recruitment of Rab5 but not of its effectors (lane 3). Further addition of hVPS34–PIK3R4 enhanced the recruitment of EEA1 and rabenosyn-5 on the proteoliposomes (lane 4), to a similar extent (EEA1), if not better (rabenosyn-5), than the recruitment on purified endosomes (lane 6). The dependency on hVPS34–PIK3R4 could be bypassed by incorporating exogenous PtdIns(3)P (0.01 mol %, lane 5) into the proteoliposomes. These results corroborate previous proposals from studies *in vitro* and *in vivo* arguing that membrane assembly of the Rab5 machinery is based on effector cooperativity[2,28].

Whereas purified early endosomes efficiently recruit Rab5 effectors from cytosol *in vitro*, proteoliposomes containing PRA1 but without SNAREs were stripped of the recruited Rab5 effectors when incubated with cytosol (not shown). Presumably, cytosol provides endogenous Rab5 effectors but also factors counter-acting the assembly process, for example, negatively acting upon Rab5 and PtdIns(3)P such as RabGDI, Rab5 GTPase-activating proteins, PtdIns(3)P-phosphatases and other molecules competing for Rab5 binding[8]. Given that both EEA1 and rabenosyn-5–hVPS45 complex can bind syntaxin 13 and syntaxin 6 on endosomes[24,26,37,38], we tested whether such interactions may contribute to the membrane recruitment of Rab5 effectors. PRA1 proteoliposomes containing either cognate syntaxin 13, VTI1A and syntaxin 6 or non-cognate t-SNAREs (where syntaxin 13 was replaced by syntaxin 7) were first incubated with the full set of recombinant Rab5 effectors except rabankyrin-5, and then further incubated with and without cytosol. Figure 2b shows that proteoliposomes containing cognate t-SNAREs recruited similar amounts of Rab5, EEA1 and rabenosyn-5–hVPS45 both in the presence and absence of cytosol (compare lane 1 with 2). In contrast, non-cognate syntaxin 7, VTI1A and syntaxin 6 proteoliposomes poorly recruited Rab5 and its effectors (especially rabenosyn-5) and incubation with cytosol completely solubilized them (lanes 3–4). Moreover, proteoliposomes containing only PRA1 and syntaxin 13 alone displayed substantial sensitivity to cytosol (lanes 5–6). These data indicate that the correct cognate SNARE complexes contribute to the recruitment and stabilization of Rab5 effectors on the membrane.

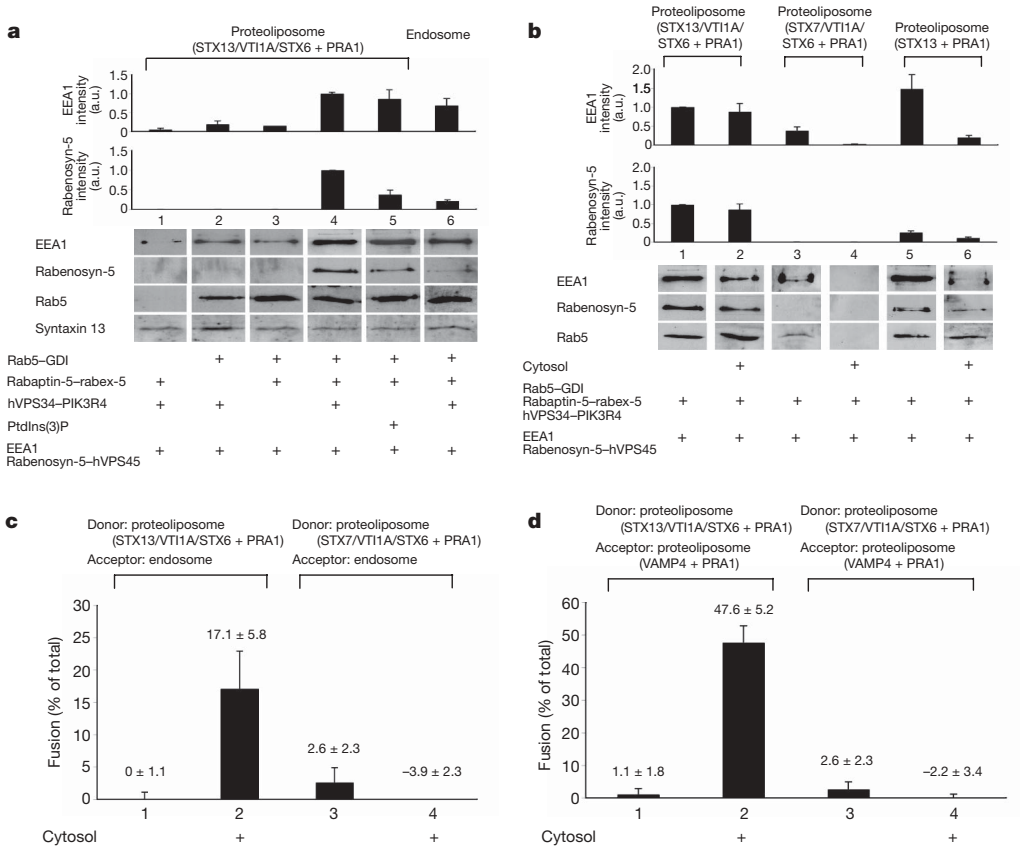

Figure 2 | Recruitment of Rab5, EEA1 and rabenosyn-5 on proteoliposomes. **a**, Proteoliposomes with a similar phospholipid and syntaxin 13 (STX13) content as early endosomes (as control, lane 6) were incubated with the indicated proteins (see Methods). Membrane-associated proteins were detected by western blotting, quantified and normalized to 1 (arbitrary units, a.u.) with the values in lane 4. **b**, Cognate t-SNAREs are necessary for the stable membrane recruitment of EEA1 and rabenosyn-5. Proteoliposomes with different SNARE sets were incubated with recombinant proteins with or without further incubation with cytosol. Membrane association was measured as in **a**. **c**, **d**, Cognate t-SNAREs are necessary for cytosol-dependent proteoliposome fusion. Membrane fusion of either cognate (lanes 1–2) or non-cognate (lanes 3–4) t-SNARE proteoliposomes with endosomes (**c**) or v-SNARE proteoliposomes (**d**) with or without cytosol was measured as in Fig. 1. Histograms show the average of three independent experiments and s.e.m.

Previous studies used proteoliposomes with a SNARE: phospholipid ratio ranging between 1:22–1:200 (refs 10, 13) and 1:500–1:2,000 (ref. 39). In our experiments, the proteoliposomes contained similar amounts of SNAREs as early endosomes (see Methods and Supplementary Fig. 4). We estimated that ~2.5 picomoles syntaxin 13 were present in the early-endosome-enriched fraction containing ~5.5 nanomoles phospholipids, resulting in a ~1:2,000 ratio. A similar ratio (~1:10,000–1:2,000, depending on the preparation) was estimated for the proteoliposomes because the concentration of syntaxin 13 and phospholipids incorporated into these membranes matched that of endosomes. The copy number of syntaxin 13 would be ~4–20 per 100 nm liposome (see Methods), the same order of magnitude of SNAREs in synaptic vesicles[40]. The concentration of syntaxin 6 was also comparable to that of endosomal fractions whereas VTI1A was present at a somewhat lower level (see Supplementary Fig. 4). VAMP4 in endosomes and proteoliposomes was barely detectable by western blotting but was not in excess over the level in endosomes.

Fusion of proteoliposomes requires cytosolic factors

We then tested the fusion of the PRA1 and t-SNARE proteoliposomes with endosomes using the same assay measuring homotypic early endosome fusion (Fig. 1). In Fig. 2c, proteoliposomes harbouring syntaxin 13, VTI1A, syntaxin 6, PRA-1 and containing biotinylated transferrin in the lumen (referred to here as donor) fused with acceptor early endosomes (containing anti-transferrin antibodies) to a comparable degree (~17.1%, lane 2) as homotypic endosome fusion (Fig. 1, lane 2), and this fusion was cytosol-dependent (compare lane 1 with 2). In contrast, donor proteoliposomes harbouring syntaxin 7, VTI1A and syntaxin 6 yielded low fusion signals that were further reduced by addition of cytosol (lanes 3 and 4), indicating that membrane fusion requires the correct cognate early endosomal t-SNARE complex[18,29].

We next attempted to substitute the acceptor endosomes with proteoliposomes containing PRA1, the cognate v-SNARE VAMP4 and anti-transferrin antibodies in the lumen. As for the endosome fusion assay, the background in the proteoliposome assay, estimated to be 5.5 ± 1.1% of the total signal, was subtracted from each measurement. Strikingly, donor proteoliposomes harbouring PRA1, syntaxin 13, VTI1A and syntaxin 6 fused with very high efficiency with acceptor proteoliposomes containing PRA1 and VAMP4 but only in the presence of cytosol (48% versus 1.1%, Fig. 2d, lanes 1 and 2) and, again, this fusion activity was dependent on the correct t-SNARE complex (compare lane 2 with 4). Thus, in this content-mixing assay, cognate SNAREs alone do not efficiently support membrane fusion.

Proteoliposome fusion requires the Rab5 machinery and SNAREs

The dependence on cytosolic factors may be accounted for, at least partially, by the Rab5 machinery. To test this hypothesis directly, we attempted to reconstitute a fully synthetic fusion reaction, using only purified recombinant components (Fig. 3a). Donor proteoliposomes with PRA1, syntaxin 13, VTI1A and syntaxin 6 incubated with acceptor proteoliposomes (PRA1, VAMP4) again yielded a very low fusion signal (1.1%). Similarly, low signals (0.9–4.6%) were obtained with proteoliposomes containing cognate SNAREs but lacking PRA1 or containing PRA1 but lacking SNAREs. Strikingly,

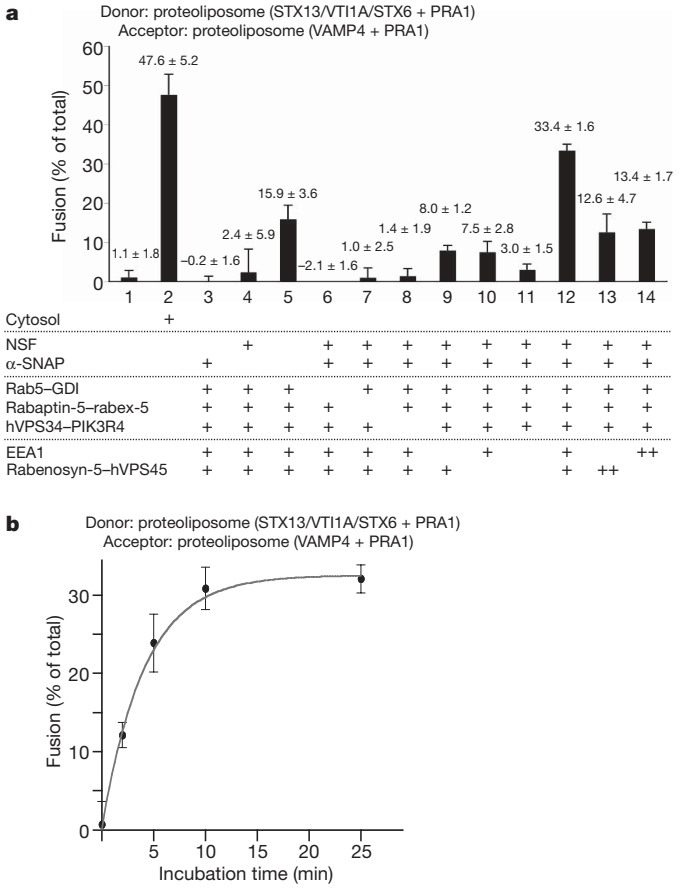

Figure 3 | The Rab5 machinery and SNAREs cooperatively promote membrane fusion. a, Donor proteoliposomes containing syntaxin 13, VTI1A, syntaxin 6 and PRA1 and acceptor proteoliposomes with VAMP4 and PRA1 were incubated without cytosol (lane 1), with cytosol (lane 2) or with the indicated recombinant proteins (lanes 3–14) at the concentration in Supplementary Table 1, as described in Methods. In lanes 13 and 14, '++' indicates the presence of 200 nM of proteins. Fusion was measured as in Fig. 1. **b**, Time course of fully synthetic proteoliposome membrane fusion. The fusion assay was carried out as in **a**, lane 12, for the indicated periods of time. Black dots, experimental data; red curve, exponential fit ($t_{1/2} = 2.8 \pm 0.7$ min). Graphs show the average of three independent experiments ± s.e.m.

the same proteoliposomes incubated with Rab5–RabGDI and the Rab5 effectors rabaptin-5–rabex-5 complex, hVPS34–PIK3R4, EEA1, rabenosyn-5–hVPS45 complex, and NSF and α-SNAP (at the concentration specified in Supplementary Table 1) at 37 °C for 25 min fused very efficiently (~33%) as shown in Fig. 3a, lane 12. The SNARE priming factors NSF and α-SNAP were required for maximal fusion signal (lanes 3–5). This is because the amount of content in the donor and acceptor liposomes allows for an increased fusion signal after multiple rounds of fusion. However, the fusion signal obtained in the absence of NSF and α-SNAP (lane 5) indicates that the t- and v-SNAREs on the separate proteoliposomes allow at least one cycle of membrane fusion without the need for priming[41]. Interestingly, omission of either α-SNAP or NSF was more inhibitory than removal of both (compare lanes 3 and 4 with 5). In the absence of NSF, surplus α-SNAP is known to bind to SNAREs non-productively[42]. NSF incorporates into high-molecular-weight oligomers with syntaxin 13, EEA1, rabaptin-5 and rabex-5 (ref. 26), but evidently without α-SNAP these complexes do not support membrane fusion. The reaction was dependent on Rab5 (lane 6), catalytic nucleotide exchange on Rab5 (lane 7) and GTP (not shown). Similar to the recruitment of Rab5 effectors (Fig. 2a), it also required the synthesis of PtdIns(3)P by hVPS34–PIK3R4 (lane 8). Note that the same complement of recombinant proteins as in lanes 6–8 supported relatively high endosome fusion (Fig. 1, lanes 6–8), probably due to residual effectors on the cellular membranes. Although either EEA1 or the rabenosyn-5–hVPS45 complex alone was necessary and sufficient for fusion (lanes 9–11), maximal fusion activity required the synergistic contribution of both Rab5 effectors (lane 12). Doubling the concentration of either effector to compensate for the loss of the other did not yield the fusion activity obtained when both were present (Fig. 3, lanes 13–14).

The fusion reaction was saturable and occurred with a $t_{1/2}$ of 2.8 ± 0.7 min (Fig. 3b). The kinetics were thus even faster than those reported for the homotypic fusion between early endosomes[35]. Altogether, these results indicate that we succeeded in reconstituting an efficient and specific proteoliposome-dependent fusion system recapitulating both the synergistic activity between components of the Rab5 machinery and the Rab- and SNARE-dependency.

Although all components in the reconstituted system are required, some exert a more regulatory role on others and, thus, can be bypassed. For example, similar to the recruitment of Rab5 effectors (Fig. 2a, b), incorporation of PtdIns(3)P into proteoliposomes bypassed the requirement for PI(3)K (Fig. 4a, lanes 3 and 4). Addition of 1 mM GTPγS in part bypassed the requirement for the rabaptin-5–rabex-5 (data not shown).

To validate the artificial proteoliposome system, we conducted a series of control experiments. For these, a 'standard full-set fusion assay' was defined as the reaction with donor and acceptor proteoliposomes and recombinant proteins as in Fig. 3a, lane 12.

First, we further tested the SNARE dependency by adding soluble syntaxin 13 or syntaxin 7 fragments lacking the transmembrane domain[26] to standard full-set fusion assays. Soluble syntaxin 13 inhibited fusion (21% of the control; Fig. 4b, lanes 1–2), whereas syntaxin 7 had a modest inhibitory effect (80% of the control, lanes 1 and 3). Altogether, these data indicate that the fusion between donor and acceptor membranes with cognate early endosome SNAREs specifically requires syntaxin 13.

Second, we verified that the immunocomplexes detected are not due to increased leakage of the luminal markers from tethered or aggregated proteoliposomes. Standard full-set fusion assays without unlabelled transferrin as the quencher were carried out, and the proteoliposomes separated into three fractions by Histodenz flotation (Fig. 4c, see Methods). As controls, donor and acceptor proteoliposomes were either directly separated without incubation or lysed after incubation before flotation. As expected, when proteoliposomes were detergent-solubilized most of the signal was detected in the bottom fraction. In contrast, most (~70%) of the cargo was detected in the top fraction for all donor, acceptor and proteoliposome products of the fusion reaction. These results indicate that the incubation does not increase content leakage from donor or acceptor proteoliposomes. Note that the luminal markers leaking from membranes are quenched by addition of excess unlabelled transferrin down to 1.1% (Fig. 3a, lane 1). In this way, we can exclude that the immunocomplexes detected in the standard full-set fusion assay are primarily due to leakage of cargo rather than membrane fusion. In fact, the signals detected are probably an under-estimate of the real fusion signal.

To rule out that fusion activity may be caused by impurities in the lipid extracts and to reconstitute membranes using a defined system, we generated artificial proteoliposomes consisting of synthetic and purified lipids (see Methods), mimicking the endosomal phospholipid content[43]. Such defined proteoliposomes with cognate t-SNAREs and PRA1 were able to fuse with equivalent lipid-defined proteoliposomes with v-SNARE and PRA1 in the presence of either cytosol or recombinant Rab5 machinery, NSF and α-SNAP (Fig. 4d).

Morphological assessment of proteoliposome fusion

Finally, to assess the fusion of proteoliposomes by an independent method, we measured the diameter and area of proteoliposomes by

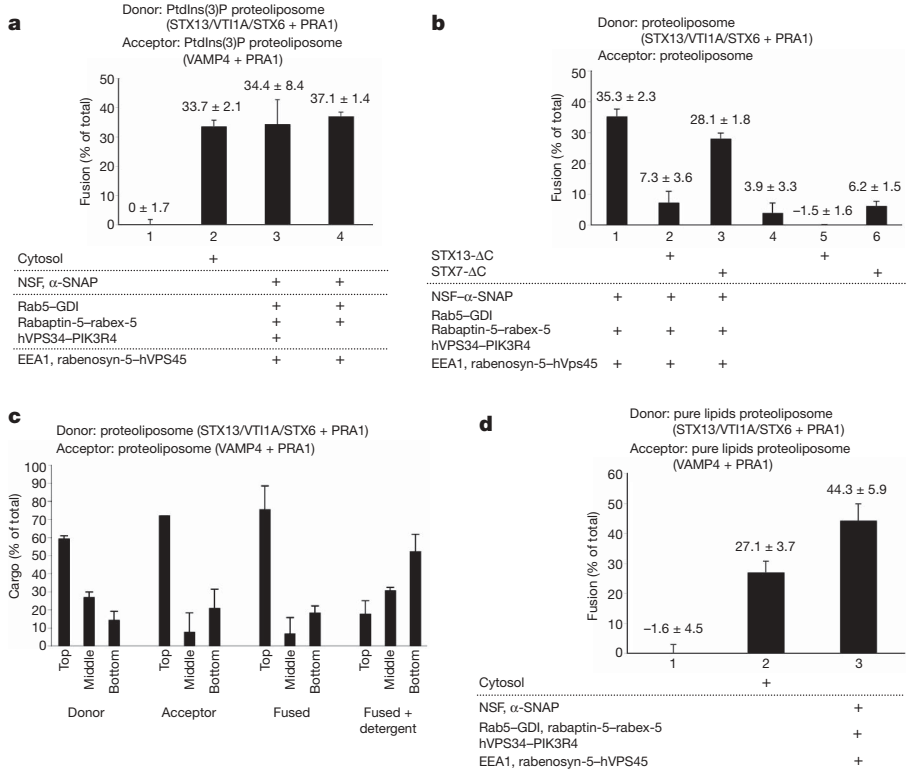

Figure 4 | Molecular requirements for membrane fusion. a, Exogenous PtdIns(3)P can bypass the requirement for PI(3)K. Proteoliposomes were supplemented with 0.01 mol % exogenous PtdIns(3)P and incubated in the absence or presence of cytosol or the indicated proteins. Fusion was measured as in Fig. 1. **b**, Requirement for SNAREs in membrane fusion assessed through the inhibitory effect of soluble syntaxin mutants. The fusion reaction (as in Fig. 3a, lane 12) was carried out in the absence or presence of 4 μM Stx13-ΔC (lanes 2 and 5) or Stx7-ΔC (lanes 3 and 6). **c**, Assessment of cargo leakage from proteoliposomes. Individual donor, acceptor or proteoliposomes incubated as in Fig. 3a, lane 12 (fused), without unlabelled transferrin were separated by Histodenz density gradient flotation and the cargo in each fraction was quantified. As a control, fused proteoliposomes were lysed before flotation (fused + detergent). **d**, Fusion between proteoliposomes reconstituted with synthetic lipids. Fusion assays with proteoliposomes consisting of pure lipids were performed as in Fig. 3a, lane 12. Data are average of three independent experiments and s.e.m.

negative staining and electron microscopy. A high number of proteins and/or protein concentrations could potentially produce membrane fragments or ruptured liposomes. We could observe, however, that donor proteoliposomes appeared as spherical vesicles (Fig. 5a). Their size ranged between ~30 and 500 nm, with most having an average diameter of ~50–100 nm (Fig. 5d). Acceptor proteoliposomes showed a similar profile (data not shown). Incubation of donor and acceptor proteoliposomes alone moderately increased the fraction of vesicles ranging from 250 to 500 nm (Fig. 5b, d), but not over 500 nm. However, incubation in the standard full-set fusion assay (Fig. 3a, lane 12) shifted the distribution profile of vesicles, yielding spherical proteoliposomes ranging between 0.5 and 1.5 μm in diameter (Fig. 5c, d). Further incubation times (for example, 24 h) did not yield significantly larger proteoliposomes over 2 μm (not shown). Using a simple mathematical model (see Supplementary Methods), we estimated that in the standard full-set fusion assay proteoliposomes undergo a minimum average of ~4.2 rounds of fusion compared with 0.17 rounds for PRA1 and SNARE-only proteoliposomes, consistent with the requirement of the Rab5 machinery, α-SNAP and NSF for maximal fusion (Fig. 3a).

We also verified that the enlarged proteoliposomes generated in the standard full-set fusion assay were indeed the products of bilayer fusion and not fusion intermediates, for example, hemifusion, by ammonium molybdenum staining and electron microscopy analysis. For donor, acceptor and fused proteoliposomes, we confirmed the bilayer membrane structure in proteoliposomes of a wide size range (Fig. 5e).

Discussion

In this study, we reconstituted the cooperative activity between the Rab5 and SNARE endosomal machinery in membrane tethering and fusion, using a combination of artificial vesicles and a set of 17 recombinant proteins. This is the first successful reconstitution of Rab-dependent membrane fusion showing the intimate interplay between Rab GTPases and SNAREs. Our results provide important mechanistic insights into membrane tethering and fusion. First, assembly of a functional Rab5 machinery requires the combinatorial activity of four different effectors (rabaptin-5–rabex-5, hVPS34–PIK3R4 PI(3)K, EEA1 and rabenosyn-5–hVPS45). Second, we could experimentally demonstrate the long-standing prediction that Rab proteins impart an additional layer of specificity on membrane tethering and fusion[2,44] to the pairing between cognate SNAREs[10]. Third, the fusion activity reconstituted here, as revealed by a bona fide content-mixing assay, used physiological concentrations of SNAREs, was even more efficient than that of early endosomes and required short incubation times. In our system, the early endosomal SNAREs proved to be very inefficient in fusing membranes (Fig. 3a), yielding signals close to background, arguing that Rab effectors together with SNAREs form a more efficient 'core machinery' than SNAREs alone.

Multiple activities may underlie the functional cooperativity between the Rab machinery and SNAREs in membrane fusion. First, one established function of Rab5 effectors is membrane tethering, as first demonstrated for EEA1 (ref. 8). This activity may help to stabilize cognate *trans*-SNAREs[26], increasing the probability to assemble fusion-competent complexes. In this respect, members of the yeast Sec1/eukaryote Munc-18 family are essential co-factors for SNAREs in membrane fusion[45,46], which for early endosomes is contributed by hVPS45 bound to rabenosyn-5 (ref. 24). Second, SNAREs contribute to the recruitment and stability of Rab5 effectors on the membrane. Third, Rab5 effectors may directly participate in membrane fusion.

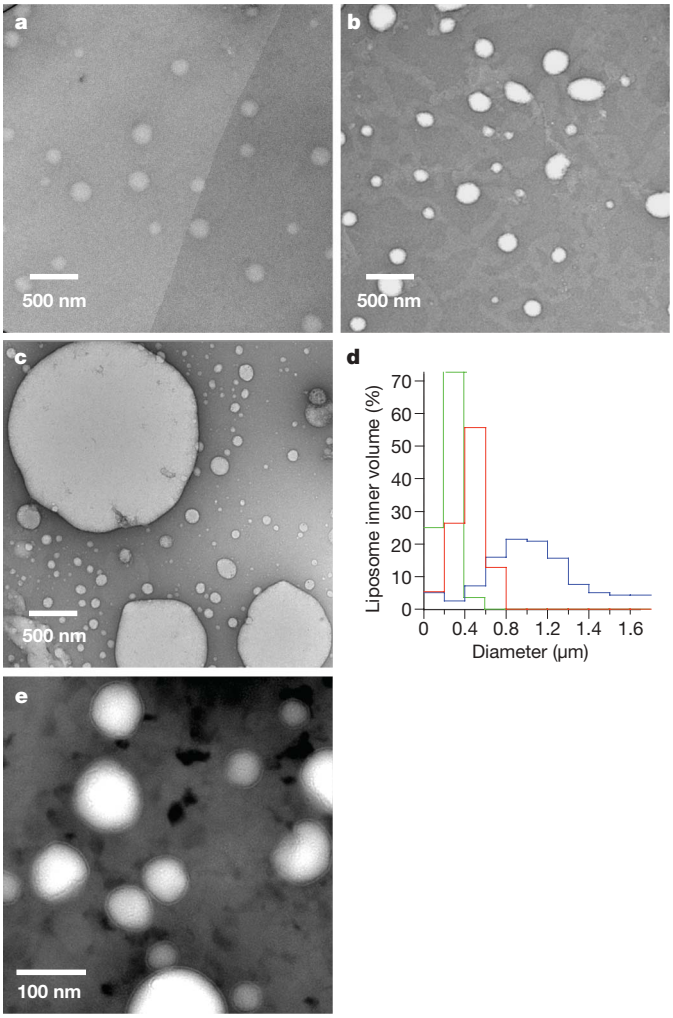

Figure 5 | Electron microscopic analysis of proteoliposomes stained with uranyl acetate (a–d) or ammonium molybdenum (e). a, Donor proteoliposomes. **b**, **c**, Donor and acceptor proteoliposomes incubated in the absence (**b**) or presence (**c**) of recombinant factors as in Fig. 3a, lane 12. **d**, Distribution of proteoliposome volumes in **a**–**c**. The histogram shows the distribution of proteoliposome volumes (as spheres calculated from the apparent diameters) normalized to 100% of the total volume of proteoliposomes measured under each experimental condition, from at least three independent preparations. Red, donor proteoliposomes as in **a**, $n = 628$; green, donor and acceptor proteoliposomes as in **b**, $n = 602$; blue, standard full-set fusion mixture of donor and acceptor proteoliposomes as in **c**, $n = 3{,}787$. **e**, Proteoliposomes after standard fusion reaction were stained with 4% ammonium molybdenum.

They may have a mechanical role by increasing lateral tension and inducing membrane curvature, as shown for synaptotagmin I (ref. 47), thus lowering the energy barrier necessary to convert the hemifusion stalk into an expanding fusion pore[12].

The reconstituted system developed here still lacks important components, such as members of the synaptotagmin family[47] and class C VPS–CORVET complex[48,49]. Some of the components used here *in vitro* may be replaced or complemented by others *in vivo*, contributing to the efficiency, specificity and regulation of membrane fusion. This synthetic biology approach could therefore be further developed towards the reconstitution of artificial organelles of increasing complexity and functional properties.

METHODS SUMMARY

Antibodies and recombinant proteins. Antibodies and the expression and purification of recombinant proteins in this Article are described in Supplementary Methods.

Proteoliposome preparation and purification. Extracted lipids from the endosome fraction of baby hamster kidney BHK cells or synthetic lipids were mixed with either PRA1 or SNARE proteins or both, in buffer containing biotinylated transferrin for t-SNARE proteoliposomes and sheep anti-transferrin antibodies for v-SNARE proteoliposomes. The mixtures were subjected to two steps of dialysis to form the proteoliposomes. Dialysed proteoliposomes were purified on a Histodenz gradient and used for protein binding and fusion studies. Details are provided in Methods.

Membrane recruitment assay. The purified proteoliposomes were incubated with recombinant proteins and the recruitment of Rab5 effectors was determined by quantitative western blotting.

Early endosome and proteoliposome fusion assays. The standard early endosome fusion assay was carried out as described previously[21]. See Methods for details. For proteoliposome fusion assays, t-SNAREs and v-SNARE proteoliposomes were purified by a two-step density-separation method, Histodenz flotation followed by sucrose gradient separation. Standard fusion assays with proteoliposomes were carried out as homotypic early endosome fusion assays except using donor proteoliposomes with acceptor proteoliposomes or endosomes (see Methods).

Electron microscopy visualization of proteoliposomes and quantification. Proteoliposomes were prepared on freshly glow-discharged carbon-coated copper grids stained with 1% uranyl acetate or 4% ammonium molybdenum. Images of the negatively stained proteoliposome specimen were collected on a TECNAI12 (FEI) electron microscope operating at 100 kV.

Full Methods and any associated references are available in the online version of the paper at www.nature.com/nature.

Received 13 February; accepted 5 May 2009.
Published online 20 May 2009.

1. Pfeffer, S. R. Transport-vesicle targeting: tethers before SNAREs. *Nature Cell Biol.* **1**, E17–E22 (1999).
2. Zerial, M. & McBride, H. Rab proteins as membrane organizers. *Nature Rev. Mol. Cell Biol.* **2**, 107–117 (2001).
3. Grosshans, B. L., Ortiz, D. & Novick, P. Rabs and their effectors: achieving specificity in membrane traffic. *Proc. Natl Acad. Sci. USA* **103**, 11821–11827 (2006).
4. Jahn, R. & Scheller, R. H. SNAREs—engines for membrane fusion. *Nature Rev. Mol. Cell Biol.* **7**, 631–643 (2006).
5. McNew, J. A. *et al.* Compartmental specificity of cellular membrane fusion encoded in SNARE proteins. *Nature* **407**, 153–159 (2000).
6. Rothman, J. E. & Sollner, T. H. Throttles and dampers: controlling the engine of membrane fusion. *Science* **276**, 1212–1213 (1997).
7. Cai, H., Reinisch, K. & Ferro-Novick, S. Coats, tethers, Rabs, and SNAREs work together to mediate the intracellular destination of a transport vesicle. *Dev. Cell* **12**, 671–682 (2007).
8. Christoforidis, S., McBride, H. M., Burgoyne, R. D. & Zerial, M. The Rab5 effector EEA1 is a core component of endosome docking. *Nature* **397**, 621–625 (1999).
9. Wang, L., Merz, A. J., Collins, K. M. & Wickner, W. Hierarchy of protein assembly at the vertex ring domain for yeast vacuole docking and fusion. *J. Cell Biol.* **160**, 365–374 (2003).
10. Weber, T. *et al.* SNAREpins: minimal machinery for membrane fusion. *Cell* **92**, 759–772 (1998).
11. Wickner, W. & Schekman, R. Membrane fusion. *Nature Struct. Mol. Biol.* **15**, 658–664 (2008).
12. Zimmerberg, J. & Gawrisch, K. The physical chemistry of biological membranes. *Nature Chem. Biol.* **2**, 564–567 (2006).
13. Schuette, C. G. *et al.* Determinants of liposome fusion mediated by synaptic SNARE proteins. *Proc. Natl Acad. Sci. USA* **101**, 2858–2863 (2004).
14. Fix, M. *et al.* Imaging single membrane fusion events mediated by SNARE proteins. *Proc. Natl Acad. Sci. USA* **101**, 7311–7316 (2004).
15. Liu, T. *et al.* SNARE-driven, 25-millisecond vesicle fusion *in vitro*. *Biophys. J.* **89**, 2458–2472 (2005).
16. Parlati, F. *et al.* Rapid and efficient fusion of phospholipid vesicles by the alpha-helical core of a SNARE complex in the absence of an N-terminal regulatory domain. *Proc. Natl Acad. Sci. USA* **96**, 12565–12570 (1999).
17. Pobbati, A. V., Stein, A. & Fasshauer, D. N- to C-terminal SNARE complex assembly promotes rapid membrane fusion. *Science* **313**, 673–676 (2006).
18. Brandhorst, D. *et al.* Homotypic fusion of early endosomes: SNAREs do not determine fusion specificity. *Proc. Natl Acad. Sci. USA* **103**, 2701–2706 (2006).
19. Sonnichsen, B. *et al.* Distinct membrane domains on endosomes in the recycling pathway visualized by multicolor imaging of Rab4, Rab5, and Rab11. *J. Cell Biol.* **149**, 901–914 (2000).
20. Barbero, P., Bittova, L. & Pfeffer, S. R. Visualization of Rab9-mediated vesicle transport from endosomes to the trans-Golgi in living cells. *J. Cell Biol.* **156**, 511–518 (2002).
21. Horiuchi, H. *et al.* A novel Rab5 GDP/GTP exchange factor complexed to Rabaptin-5 links nucleotide exchange to effector recruitment and function. *Cell* **90**, 1149–1159 (1997).

22. Christoforidis, S. *et al.* Phosphatidylinositol-3-OH kinases are Rab5 effectors. *Nature Cell Biol.* **1,** 249–252 (1999).
23. Shin, H. W. *et al.* An enzymatic cascade of Rab5 effectors regulates phosphoinositide turnover in the endocytic pathway. *J. Cell Biol.* **170,** 607–618 (2005).
24. Nielsen, E. *et al.* Rabenosyn-5, a novel Rab5 effector, is complexed with hVPS45 and recruited to endosomes through a FYVE finger domain. *J. Cell Biol.* **151,** 601–612 (2000).
25. Schnatwinkel, C. *et al.* The Rab5 effector Rabankyrin-5 regulates and coordinates different endocytic mechanisms. *PLoS Biol.* **2,** 1363–1380 (2004).
26. McBride, H. M. *et al.* Oligomeric complexes link Rab5 effectors with NSF and drive membrane fusion via interactions between EEA1 and syntaxin 13. *Cell* **98,** 377–386 (1999).
27. Hoepfner, S. *et al.* Modulation of receptor recycling and degradation by the endosomal kinesin KIF16B. *Cell* **121,** 437–450 (2005).
28. Del Conte-Zerial, P. *et al.* Membrane identity and GTPase cascades regulated by toggle and cut-out switches. *Mol. Syst. Biol.* **4,** 206 (2008).
29. Zwilling, D. *et al.* Early endosomal SNAREs form a structurally conserved SNARE complex and fuse liposomes with multiple topologies. *EMBO J.* **26,** 9–18 (2007).
30. Bhalla, A., Chicka, M. C., Tucker, W. C. & Chapman, E. R. Ca^{2+}-synaptotagmin directly regulates t-SNARE function during reconstituted membrane fusion. *Nature Struct. Mol. Biol.* **13,** 323–330 (2006).
31. Dennison, S. M., Bowen, M. E., Brunger, A. T. & Lentz, B. R. Neuronal SNAREs do not trigger fusion between synthetic membranes but do promote PEG-mediated membrane fusion. *Biophys. J.* **90,** 1661–1675 (2006).
32. Starai, V. J., Jun, Y. & Wickner, W. Excess vacuolar SNAREs drive lysis and Rab bypass fusion. *Proc. Natl Acad. Sci. USA* **104,** 13551–13558 (2007).
33. Ullrich, O., Horiuchi, H., Bucci, C. & Zerial, M. Membrane association of Rab5 mediated by GDP-dissociation inhibitor and accompanied by GDP/GTP exchange. *Nature* **368,** 157–160 (1994).
34. Mayer, A., Wickner, W. & Haas, A. Sec18p (NSF)-driven release of Sec17p (α-SNAP) can precede docking and fusion of yeast vacuoles. *Cell* **85,** 83–94 (1996).
35. Rybin, V. *et al.* GTPase activity of Rab5 acts as a timer for endocytic membrane fusion. *Nature* **383,** 266–269 (1996).
36. Sivars, U., Aivazian, D. & Pfeffer, S. R. Yip3 catalyses the dissociation of endosomal Rab–GDI complexes. *Nature* **425,** 856–859 (2003).
37. Simonsen, A., Gaullier, J. M., D'Arrigo, A. & Stenmark, H. The Rab5 effector EEA1 interacts directly with syntaxin-6. *J. Biol. Chem.* **274,** 28857–28860 (1999).
38. Ungermann, C., Price, A. & Wickner, W. A new role for a SNARE protein as a regulator of the Ypt7/Rab-dependent stage of docking. *Proc. Natl Acad. Sci. USA* **97,** 8889–8891 (2000).
39. Mima, J. *et al.* Reconstituted membrane fusion requires regulatory lipids, SNAREs and synergistic SNARE chaperones. *EMBO J.* **27,** 2031–2042 (2008).
40. Takamori, S. *et al.* Molecular anatomy of a trafficking organelle. *Cell* **127,** 831–846 (2006).
41. Weber, T. *et al.* SNAREpins are functionally resistant to disruption by NSF and alphaSNAP. *J. Cell Biol.* **149,** 1063–1072 (2000).
42. Collins, K. M. & Wickner, W. T. Trans-SNARE complex assembly and yeast vacuole membrane fusion. *Proc. Natl Acad. Sci. USA* **104,** 8755–8760 (2007).
43. Kobayashi, T. *et al.* A lipid associated with the antiphospholipid syndrome regulates endosome structure and function. *Nature* **392,** 193–197 (1998).
44. Pfeffer, S. & Aivazian, D. Targeting Rab GTPases to distinct membrane compartments. *Nature Rev. Mol. Cell Biol.* **5,** 886–896 (2004).
45. Dulubova, I. *et al.* Munc18–1 binds directly to the neuronal SNARE complex. *Proc. Natl Acad. Sci. USA* **104,** 2697–2702 (2007).
46. Shen, J. *et al.* Selective activation of cognate SNAREpins by Sec1/Munc18 proteins. *Cell* **128,** 183–195 (2007).
47. Martens, S., Kozlov, M. M. & McMahon, H. T. How synaptotagmin promotes membrane fusion. *Science* **316,** 1205–1208 (2007).
48. Rink, J., Ghigo, E., Kalaidzidis, Y. & Zerial, M. Rab conversion as a mechanism of progression from early to late endosomes. *Cell* **122,** 735–749 (2005).
49. Peplowska, K. *et al.* The CORVET tethering complex interacts with the yeast Rab5 homolog Vps21 and is involved in endo-lysosomal biogenesis. *Dev. Cell* **12,** 739–750 (2007).

Supplementary Information is linked to the online version of the paper at www.nature.com/nature.

Acknowledgements We are grateful to K. Simons and B. Hoflack for discussions, to C. Stroupe and W. Wickner for sharing unpublished information, and to G. Marsne, I. Baines, W. Huttner, K. Simons, C. Stroupe and W. Wickner for critical reading of the manuscript. We acknowledge support by the systems biology network HepatoSys of the German Ministry for Education and Research (BMBF, grant 0313082J), the EU Integrated Project EndoTrack, the DFG and the Max Planck Society (including the Max Planck Partner Group grant to M.Z. and M.M.). T.O. was supported by The Nakatomi Foundation.

Author Contributions M.M. conducted the initial studies and tested the recombinant proteins in endosome fusion and the membrane recruitment of Rab5 and its effectors on proteoliposomes, and B.L. further developed such a proteoliposome system. D.D. and A.R. established several of the protocols of purification of recombinant proteins. T.O. completed the development of these procedures and conducted all biochemical experiments on membrane fusion reported in this study. Ü.C. performed the electron microscopy analysis, Y.K. did the statistical analysis and the mathematical model of membrane fusion, and M.Z. conceived and directed the project and wrote the manuscript with the help of T.O., M.M. and Y.K.

Author Information Reprints and permissions information is available at www.nature.com/reprints. Correspondence and requests for materials should be addressed to M.Z. (zerial@mpi-cbg.de).

METHODS

Antibodies. Rabbit polyclonal anti-EEA1 and anti-rabenosyn-5 antibodies were previously described[24], as well as anti-Rab5 and anti-syntaxin 13 (ref. 26).

Expression and purification of recombinant proteins. The expression and purification of recombinant proteins in this Article are described in Supplementary Methods.

Proteoliposome preparation. Early-endosome-enriched fractions from baby hamster kidney (BHK-21) cells were prepared as described[43]. Lipids were extracted from using chloroform/methanol (2:1, v/v), dried by nitrogen stream and dissolved in liposome buffer, 20 mM Hepes/OH, pH 7.5, 1% CHAPS and 500 mM KCl for t-SNARE (syntaxin 6, VTI1A and syntaxin 13 or syntaxin 7) proteoliposomes, and the same buffer containing 300 mM KCl for v-SNARE (VAMP4) proteoliposomes. For the incorporation of exogenous PtdIns(3)P into proteoliposomes, 0.01 mol % of synthetic PtdIns(3)P was added to the lipid extract from the BHK endosome fraction in chloroform/methanol solution. The reconstitution of proteoliposomes with synthetic and purified phospholipids (Avanti Polar Lipids) followed the same protocol as above except that 96 nanomoles of PC (48 mol %), 50 nanomoles of PE (25 mol %), 18 nanomoles of SM (9 mol %), 18 nanomoles of PS (9 mol %) and 18 nanomoles of PI (9 mol %) were dissolved in 4 ml of chloroform/methanol (2:1, v/v). Either recombinant His_6-tagged PRA1 (final 500 nM) or SNARE proteins (each final 10 nM) or both were added to 120 µl of lipid solution (1 mM phospholipids) containing biotinylated transferrin (final 250 µg ml^{-1}) for t-SNARE proteoliposomes and sheep anti-transferrin antibodies (Scottish Antibody Production Unit, final 75 µg ml^{-1}) for v-SNARE proteoliposomes. Each mixture was incubated with gentle agitation in the dark at room temperature. Next, 120 µl of the t-SNARE mixture was first dialysed against 12 ml of dialysis-500 buffer (25 mM Hepes/OH, pH 7.5, 500 mM KCl) with 20 µg ml^{-1} holo-transferrin (Sigma) for 12–15 h in the dark at 4 °C, followed by a second dialysis against 120 ml of dialysis-500 buffer for 4 h in the dark to remove CHAPS. In the case of v-SNARE proteoliposomes, the mixture was subjected to two steps of dialysis as above in dialysis-300 buffer (25 mM Hepes/OH, pH 7.5, 300 mM KCl), with the first step supplemented with 4.5 µg ml^{-1} sheep anti-transferrin antibodies.

Proteoliposome purification and lipid quantification. Proteoliposomes were purified by Histodenz density gradient centrifugation. Dialysed t-SNARE proteoliposomes were mixed gently with 360 µl of 48% Histodenz buffer (48% Histodenz, 1 mM GTP, 100 µM $CaCl_2$ and 300 mM KCl in fusion buffer, see below) and then covered with 400 µl of 25% Histodenz buffer and 160 µl of Histodenz-free buffer, followed by centrifugation in a TLS-55 rotor (Beckman) at 100,000*g* for 1 h at 4 °C. Fractions of 40 µl were collected from the top to the bottom of the gradient and SNARE-enriched fractions, as determined by western blot analysis, at the interphase between the first and the second phases (fourth fraction from the top) were selected for protein-binding studies. The phospholipid concentration of proteoliposomes in this fraction was about ~2.5 mM, as quantified by the Bartlett assay[50].

Membrane recruitment assay. The protein recruitment assay was performed in the fusion buffer containing 12.5 mM Hepes/OH, pH 7.4, 1.5 mM magnesium oxaloacetate, 75 mM potassium acetate, 3 mM imidazole and 1 mM DTT[21]. The purified proteoliposomes (1 mM phospholipid) were incubated with recombinant proteins in the presence of an ATP-regeneration system, 1 µM $CaCl_2$ and 30 µM GTP in a total volume of 20 µl fusion buffer at 37 °C for 25 min. Recombinant proteins were adjusted to the final concentrations indicated in Supplementary Table 1. When the effect of cytosol was evaluated, samples were supplemented with HeLa cytosol (final concentration 3 mg ml^{-1}) and further incubated at 37 °C for 25 min. The reaction was arrested by transferring the sample on ice. Samples were then supplemented up to 35 µl with fusion buffer, followed by purification again by flotation on Histodenz density gradient consisting of 105 µl of 48%, 80 µl of 25% and 30 µl of Histodenz-free buffer, followed by fractionation as above. The floated fractions (top 50 µl) were used for testing the recruitment of Rab5 effectors as determined by quantitative western blotting using recombinant proteins as standards.

Membrane fusion assays. Standard early endosome fusion assay was carried out as previously described[21]. In brief, 'donor' and 'acceptor' endosomes were purified from HeLa cells that had internalized either biotinylated human transferrin or sheep anti-transferrin antibodies, respectively, for 5 min. Both endosome-enriched fractions were mixed with excess unlabelled transferrin (2 mg ml^{-1}), an ATP-regenerating system and incubated with 3 mg ml^{-1} HeLa cytosol at 37 °C for 25 min (see Supplementary Fig. 2a). Membranes were solubilized in 2% Triton X-100 buffer at room temperature for 1 h and the resulting immunocomplexes between biotinylated transferrin and anti-transferrin antibodies were immobilized onto streptavidin-coated 96-well plates and detected by a rabbit anti-sheep secondary antibody coupled to MSD SULFO-TAG (ruthenium (II) tris-bipyridine) in an electrochemical reaction using the SECTOR Imager 6000 (MSD). In this system the electrochemical reaction is initiated when current is applied to the plates. In combination with the co-reactant tripropylamine, which is contained in the read buffer, the MSD SULFO-TAG emits light (620 nm) that is detected by a highly sensitive CCD camera. Background signals are minimal because the stimulus (electricity) is decoupled from the signal (light). Multiple excitation cycles of each label amplify the signal to enhance light levels and improve sensitivity. Detection limits may be as low as 10^6 molecules with a dynamic range of 6 logs. In our system, a few femtomoles of immunocomplexes could be detected (see Supplementary Fig. 2b, c). To quantify the maximal possible fusion signal (total), mixed acceptor and donor endosomes in each assay were solubilized in the absence of unlabelled transferrin and the resulting immunocomplex was quantified as described above. This value was considered as 100%. In this study, acceptor endosomes (final concentration in the assay, 80 µM phospholipids) and donor endosomes (final concentration, 40 µM phospholipids) were mixed in a total volume of 20 µl fusion buffer supplemented with 1 µM $CaCl_2$ and 30 µM GTP as a standard. When testing purified recombinant proteins instead of cytosol in the homotypic endosome fusion assay, the final concentration of each indicated recombinant protein was adjusted to the value indicated in Supplementary Table 1.

For the fusion assay with synthetic proteoliposomes, t-SNARE and v-SNARE proteoliposomes were purified by a two-step density-separation method. For t-SNARE proteoliposomes, the first step was done by flotation on a Histodenz gradient, in the same way as for the membrane recruitment assay. The top 240 µl fraction was sequentially mixed with an equal volume of 62% sucrose buffer (62% sucrose, 3 mM imidazole and 300 mM KCl). The proteoliposome mixture was covered with 200 µl of 35% sucrose buffer, 150 µl of 25% sucrose buffer and 50 µl of 8.5% sucrose buffer, followed by centrifugation in a TLS-55 rotor at 100,000*g* at 4 °C for 1 h. Fractions of 40 µl were collected from the top to the bottom of the gradient, and the SNARE-enriched fractions were determined as described above (usually seventh or eighth fraction from the top; Supplementary Fig. 4) and used as the 'donor' in the fusion assay. The purification of v-SNARE proteoliposomes was also carried out in the same way, except that KCl was omitted in both density gradient separation processes. The final fraction was used as the 'acceptor' in the fusion assay. The levels of SNARE proteins in the donor or acceptor proteoliposomes purified by sucrose density gradient were estimated by quantitative western blot analysis using recombinant proteins as standards and compared with those in endosomes (adjusted to obtain comparable amounts according to the phospholipid content). For example, we estimated that ~1.0 picomoles syntaxin 13 were present in the proteoliposomes containing ~2.2 nanomoles phospholipids, resulting in a molar ratio ranging between ~1:10,000 and 1:2,000, depending on the preparation and the error in the measurement. Assuming that a 40 nm vesicle contains ~7,000 phospholipids[40] covering 50% of the surface of the membrane (the other 50% being covered by transmembrane proteins and non-phospholipids, that is, cholesterol), we estimated that the copy number of syntaxin 13 ranges between ~4 and 20 in a 100 nm proteoliposome (correcting for 6.25 times the surface area).

Calibration experiments were conducted to find the optimal ratio between donor and acceptor proteoliposomes. First, the concentration of donor proteoliposomes (containing biotinylated transferrin) was adjusted to yield half maximal intensity of the total signal generated upon solubilization and incubation with excess of anti-transferrin antibodies. Similarly, the concentration of acceptor proteoliposomes (containing anti-transferrin antibodies) was adjusted to yield half maximal intensity of the total fusion signal obtained upon solubilization with donor proteoliposomes at the selected concentration. This corresponded to three times higher concentration of donors than acceptors. For this, donor proteoliposomes (final concentration in the assay, 75 µM phospholipids) and acceptor proteoliposomes (final concentration, 25 µM phospholipids) were mixed in the fusion assay. Standard fusion assays with proteoliposomes were also carried out with unlabelled transferrin, an ATP-regeneration system, 1 µM $CaCl_2$ and 30 µM GTP at 37 °C for 25 min. No addition or addition of 100 µM $CaCl_2$ did not result in significant differences in fusion signal (Supplementary Fig. 5).

For the experiments of proteoliposome–endosome fusion, donor proteoliposomes (final concentration, 75 µM phospholipids) were mixed with acceptor endosomes (final concentration, 80 µM phospholipids).

In the endosome fusion assay with cytosol, ~1,500 electrochemiluminescence (ECL) units of emission signal were detected as an endosome fusion activity and ~6,000 ECL units as a total using 0.8 nanomoles phospholipids in donor and 1.6 nanomoles phospholipids in acceptor endosomes. They corresponded to 4.2 femtomoles and 17.5 femtomoles of biotinylated transferrin and anti-transferrin antibodies, respectively (Supplementary Fig. 2). In the fusion between proteoliposomes, we obtained ~1,000 ECL units as a fusion activity in the presence of cytosol (Fig. 3a, lane 2) and ~2,000 ECL units as a total using 1.5 nanomoles phospholipids in donor and 0.5 nanomoles phospholipids in acceptor proteoliposomes. They corresponded to 1.5 femtomoles and 4.3

femtomoles of immunocomplex, respectively (Supplementary Fig. 2). Concerning the cargo, in endosomes, the estimated molecular ratio of biotinylated transferrin to phospholipids was ~1:90,000, and that of anti-transferrin antibody to phospholipids was ~1:45,000. The estimated molecular ratio of biotinylated transferrin to phospholipids in donor proteoliposomes was ~1:300,000, and that of anti-transferrin antibody in acceptor proteoliposomes was ~1:100,000. Soluble truncated mutants of syntaxin 13 (Stx13-ΔC: 1–234 amino acids) or syntaxin 7 (Stx7-ΔC: 1–217 amino acids) lacking the transmembrane domains were expressed and purified as previously described[26]. Soluble syntaxins (4 μM) were added to the standard fusion assay mixtures with endosome or proteoliposomes immediately before starting incubation at 37 °C for 25 min.

Proteoliposome flotation assay. The proteoliposome fusion reaction was carried out in the absence of unlabelled transferrin like a standard fusion assay with recombinant Rab5 machinery, NSF and α-SNAP proteins in the concentrations described in Supplementary Table 1. The reaction mixture (20 μl) was adjusted to 30 μl with fusion buffer and mixed with 90 μl of 48% Histodenz buffer, and then covered with 100 μl of 25% Histodenz buffer and 40 μl of Histodenz-free buffer, followed by centrifugation in a TLS-55 rotor (Beckman) at 100,000*g* at 4 °C for 1 h. The 'top' 120 μl, 'middle' 60 μl and the 80 μl at the 'bottom' were taken, solubilized in 2% Triton X-100 buffer and the resulting complex between biotinylated transferrin and anti-transferrin antibodies was quantified as described above. As control experiments, the same volume of donor and acceptor were adjusted to 30 μl with fusion buffer and subjected to Histodenz gradient flotation. Each donor fraction was incubated with 200 picomoles of anti-transferrin antibodies in 2% Triton X-100 at room temperature for 1 h. For acceptor membrane, 100 picomoles of biotinylated transferrin were pre-incubated with streptavidin immobilized in the MSD plate. Each acceptor fraction was also solubilized in 2% Triton X-100 buffer at room temperature for 15 min, and then further incubated with biotinylated transferrin pre-fixed on the MSD plate at room temperature for 1 h. The immunocomplex detection was carried out as described above. As a negative control, fused proteoliposomes were solubilized in 2% Triton X-100 immediately after the fusion reaction and subjected to Histodenz gradient flotation, followed by the quantification of their cargo in each fraction.

Electron microscopy visualization and quantification of proteoliposomes. Proteoliposomes were prepared on freshly glow-discharged carbon-coated copper grids stained with 1% uranyl acetate or 4% ammonium molybdenum. Images of the negatively stained proteoliposome specimen were collected on a TECNAI12 (FEI) electron microscope operating at 100 kV. Fusion reaction in the presence or absence of recombinant NSF, α-SNAP and Rab5 machinery proteins was carried out as a standard full-set fusion assay.

To provide an unbiased quantification, electron microscopy images were analysed using the MotionTracking software[48] to automatically recognize and statistically analyse the parameters of proteoliposomes. In brief, the images were smoothed by bilateral filter and proteoliposomes were identified by two algorithms: watershed algorithm for vesicles with diameter above 200 nm, and base-function fitting for objects smaller than 200 nm. The results of the identification were verified manually and are shown in Fig. 5d for 628 donor or acceptor proteoliposomes, donor and acceptor proteoliposomes containing PRA1 and cognate v- and t-SNAREs incubated at 37 °C for 25 min in the absence (602) and presence (3,787) of the full set of proteins.

Estimation of average number fusion rounds per proteoliposome. The number of fusion rounds was inferred from the mean volume of the proteoliposomes on the basis of the model described in the Supplementary Methods.

50. Bartlett, G. R. Colorimetric assay methods for free and phosphorylated glyceric acids. *J. Biol. Chem.* **234**, 469–471 (1959).